

## Effect of Laser Parameters on the Corrosion Resistance of the ASTM F139 Stainless Steel

*Eurico Felix Pieretti\**, *Elisabete Jorge Pessine*, *Olandir Vercino Correa*, *Wagner de Rossi*,  
*Maurício David Martins das Neves*

Instituto de Pesquisas Energéticas e Nucleares (IPEN/CNEN), Av. Prof. Lineu Prestes 2242, Cidade Universitária, São Paulo – SP, 05508-000, Brazil

\*E-mail: [efpieretti@usp.br](mailto:efpieretti@usp.br)

*Received:* 19 October 2014 / *Accepted:* 14 November 2014 / *Published:* 16 December 2014

---

The investigation on the corrosion resistance of biomaterials and the effects of manufacturing processes, including marking for traceability, is extremely important to evaluate whether the surface modification caused by marking affects the properties of the biomaterial. The engraving process by laser beam has been used to ensure the identification and traceability of orthopedic implants. This study evaluates the influence of the laser marking parameters, specifically the pulse energy and engraving rate, on the corrosion resistance of the ASTM F139 austenitic stainless steel, after engraving with Nd: YAG laser beam by means of electrochemical methods. The electrolyte used was a phosphate buffered solution, with pH 7.4, and 37 °C. The results showed that the laser marking parameters affect the protective properties of the passive film and influence the susceptibility to corrosion of this biomaterial.

---

**Keywords:** Biomaterials, stainless steel, corrosion, laser marks.

### 1. INTRODUCTION

Material's surfaces for implantable applications ought to be suitable for their performance, so it's important to study their surface finish, which increases with regard to the adhesion system between the biomaterial and the adjacent tissue [1].

To preserve the integrity of the device, as well as the tissues and organs adjacent to it, thereby ensuring a better quality of life for the patients, it is necessary that the mechanical properties do not change throughout its useful life, or at least remain stable during a prolonged period of use [2].

Orthopedic implants are designed and constructed so that, when used under the conditions and for the purposes intended, do not compromise the clinical condition or safety of the patients. The

implants can be divided into two categories: devices for temporary or permanent fixation. The purpose of fixation devices is temporary fracture stabilization of the bone to its natural healing; already securing devices are permanently implanted in place of the fractured bone, replacing it [3].

To facilitate selection testing of a material suitable for implantation, one must consider the nature of the biomaterial contact with the region of the body where it is used and the duration of contact [4].

The last step of the implants manufacturing process is the surface treatment, which can include hardening, polishing, sandblasting, marking and passivation.

According to Pourbaix et al. [5], the surface treatment can influence local bone response, bone healing or even lack thereof, and the fatigue strength of the implants. This local bone response of metallic implants is affected by corrosion, in turn, can be affected by the presence of foreign particles, surface finish and other factors.

The storage location of implants must be a region of low stress concentration and should not cross the edges of holes or edges countersinking of the implant, is indicated in the design of the implant [6].

The surface finish of the implant is of fundamental importance because it ensures that the same will perform their function properly, for example, a metallic biomaterial which is cemented within the bone requires a rougher surface finish, and on the other hand, sometimes the same biomaterial needs of a region with smoother finish.

In general, roughness is required for greater adhesion and fixation, since the finer finish, smooth and polished is desired for movable joints of the body, typically these are replaced by sets containing metallic - polymeric biomaterials, ceramics - metallic, or, metallic - composites. The characteristics of the surface finish various affects factors relating to the properties of biomaterials, including hardness, wear, friction and corrosion resistance [7-9].

The influence of the roughness on the corrosion resistance is generally related to the fact that the number of pits in a metastable smoother surface is lower than that found in rougher surfaces [8], i.e. a smoother surface finish and more homogeneous reduces the incidence of metastable pitting substantially by reducing the number of sites able to be activated in the growth of metastable pits.

Surface finishing treatment by laser techniques has been widely used for metallic biomaterials that provide advantages towards other methods because this allows a high degree of automation, high scanning speed, excellent reproducibility, high durability, does not give rise to wear in the tooling and allows recording symbols with complex geometries even on uneven surfaces [10 - 15]. Laser marking process ensures all the characteristics cited above, although produce regions essentially associated with anodic sites diminishing its corrosion resistance, even in solutions containing proteins [16 – 19].

The aim of this work was to evaluate the effect of a nanosecond Nd: YAG laser treatment on the surface finishing of the ASTM F 139 stainless steel by roughness measurements and electrochemical tests. This investigation is important because indicates which laser parameter most affects electrochemical behaviour of this biomaterial.

## 2. EXPERIMENTAL

Samples of the ASTM F 139 austenitic stainless steel, with the composition (wt. %): 0.38 Si, 2.09 Mn, 0.026 P, 2.59 Mo, 18.32 Cr, 14.33 Ni, 0.023 C, 0.0003 S, and Fe balance, were prepared in the form of rolled plates with the dimensions: 72.0 mm x 17.0 mm x 1.5 mm. Laser marking was carried out using a pulsed Nd: YAG laser, at wavelength of 1064 nm, with 20 Hz of frequency and scanning speeds of 4 mm/s and 8 mm/s with pulse intensities of 0.05 J and 0.35 J, as shown in Table 1.

**Table 1.** Laser treatment parameters used for each surface finishing.

Surface finishing (sample)	Scan rate (mm/s)	Pulse energy (J)
1	4	0.05
2	4	0.35
3	8	0.05
4	8	0.35

To evaluate the topographic roughness was used a scanning electron microscope (SEM) with low vacuum tungsten filament and closest approach of  $10 \times 10^5$  times, brand: Hitachi, model: TM3000 with software for data acquisition: topographic 3D Viewer.

The corrosion resistance evaluation of this biomaterial was carried out by electrochemical techniques, specifically, monitoring the open circuit potential (OCP) for 17 h and electrochemical impedance spectroscopy (EIS). All electrochemical tests were carried out using a three electrode cell set-up, with a Pt counter electrode (wire with geometric area of 2.0 cm<sup>2</sup>) and an Ag/AgCl reference electrode (3M), using a Gamry PCI4/300 equipment and an aerated phosphate buffered saline (PBS) solution, prepared from high purity chemical reagents and deionized water, containing NaCl 8.8 g/L, KCl 0.2 g/L, Na<sub>2</sub>HPO<sub>4</sub> 1.15 g/L, KH<sub>2</sub>PO<sub>4</sub> 0.2 g/L, with a pH value of 7.4 and a conductivity of 15.35 mS, at  $(37 \pm 1)$  °C.. The area of the working electrode exposed to the electrolyte was 1 cm<sup>2</sup>. In order to evaluate reproducibility of results, four samples were tested for each surface condition investigated. The experimental EIS data were adjusted to an equivalent electric circuit (EEC), for every kind of surface tested.

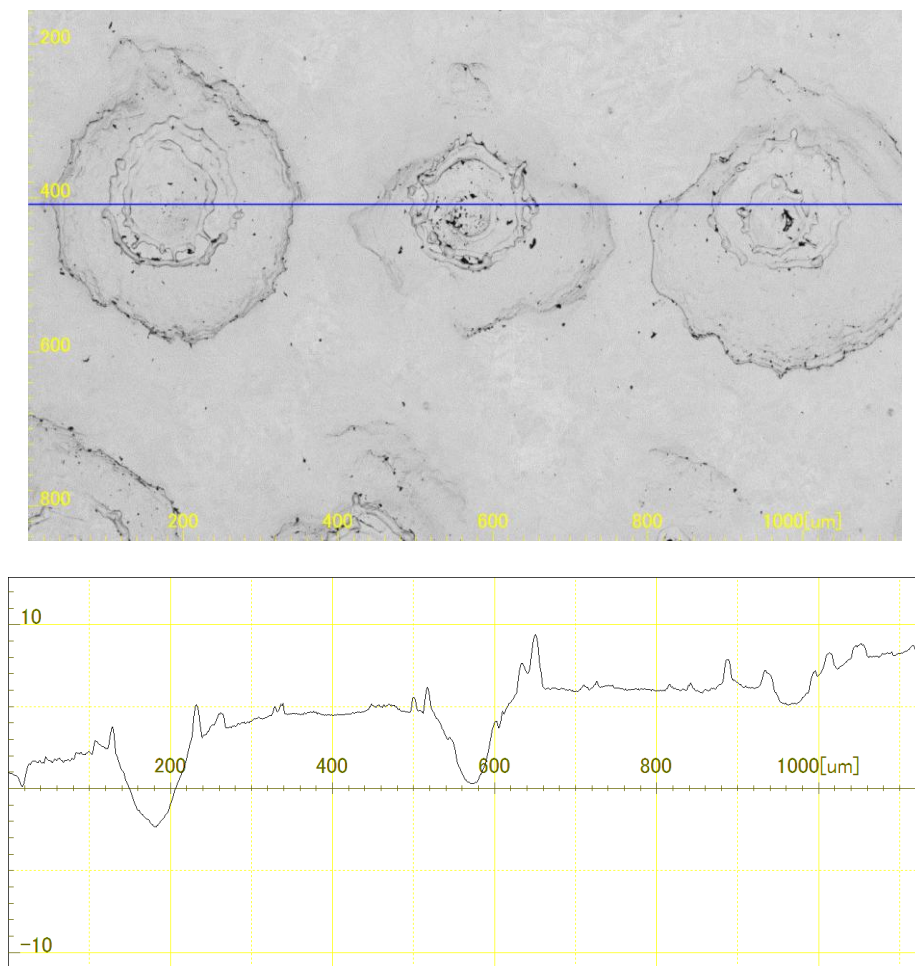
## 3. RESULTS AND DISCUSSION

### 3.1. Surface finishing analysis

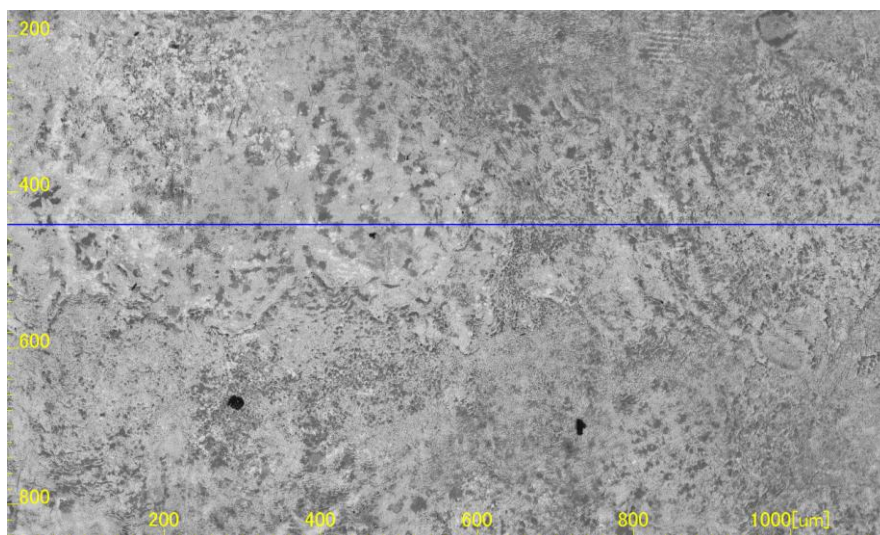
The surface finish of the samples is strongly influenced by the variation of the intensity of the laser beam pulse. The images below show this effect. Figure 1 shows the effect of the laser beam pulses on the topography of the samples, such as differences in height and depth in relation to adjacent

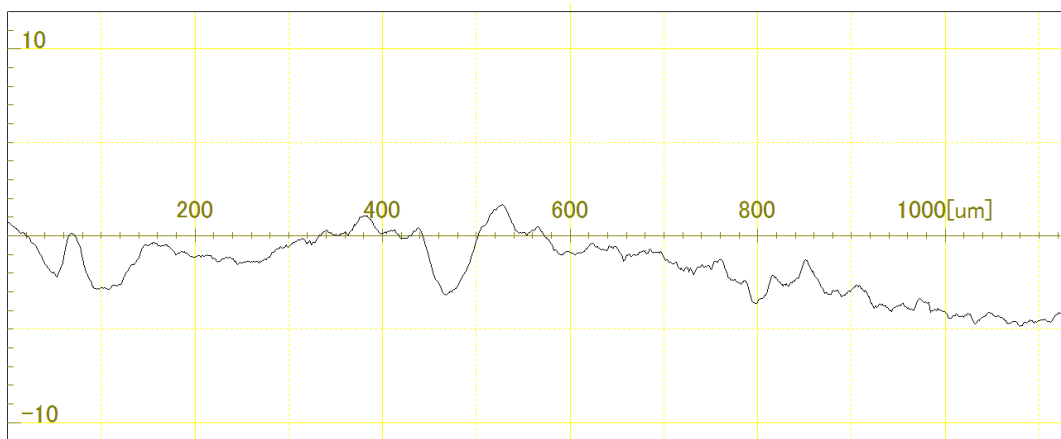
areas; peaks and spills resulting from melting of the surface of this biomaterial. It is possible to verify the melting of the base material with removal of molten metal in the region of incidence of the laser beam, which modifies the roughness of these surfaces.

Figure 1 also presents roughness profiles of the regions treated by laser, where the influence on the topography of the samples submitted to the Nd:YAG laser beam is more evident.

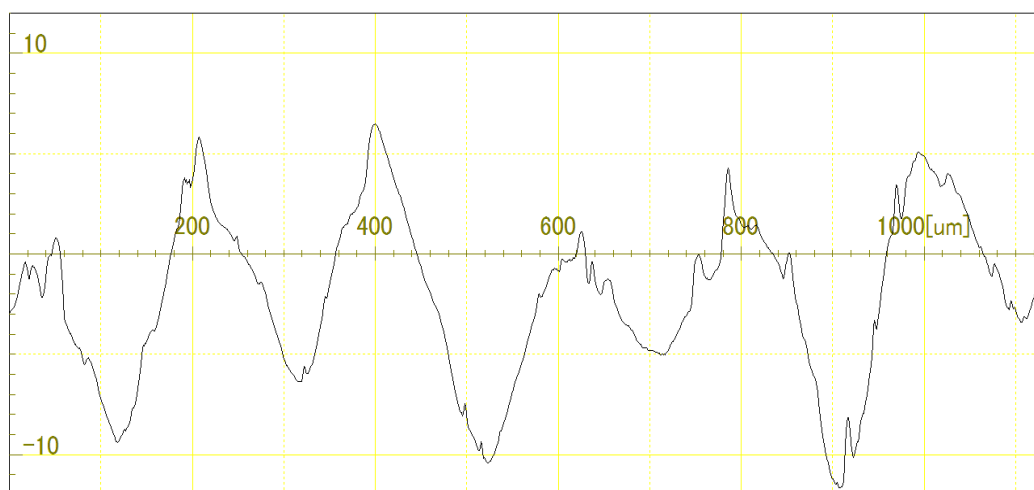
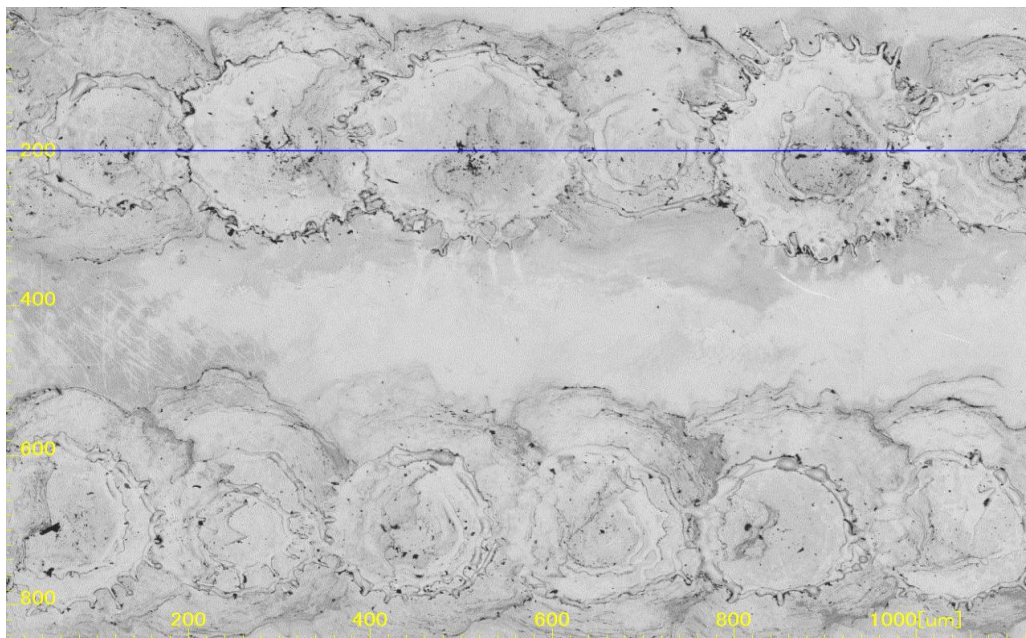


(a) E= 0.05 J and V= 4mm/s.





(b)  $E= 0.35$  J and  $V= 4$ mm/s.



(c)  $E= 0.05$  J and  $V= 8$ mm/s.

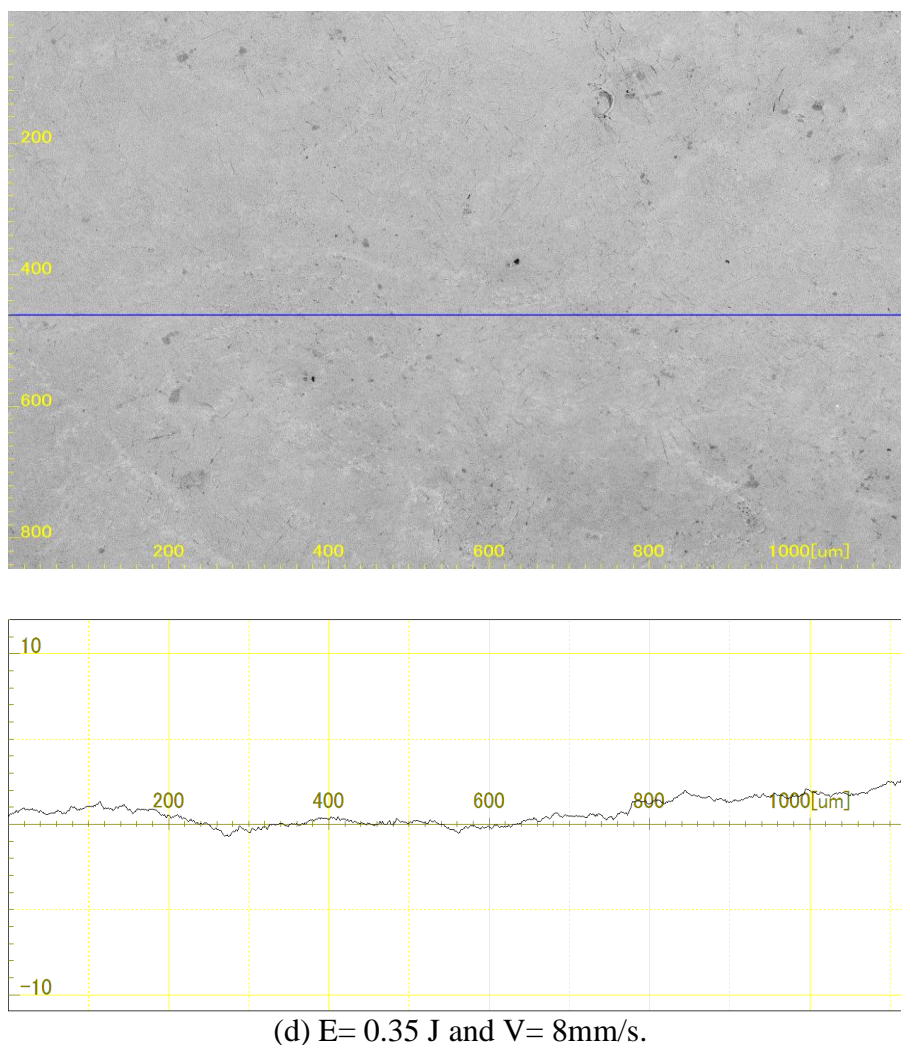


**Figure 1.** SEM images presenting the surface finishing of testes samples and roughness profiles of the biomaterial’s samples with laser treatment made by using different parameters, showing topographical changes. The blue line indicates the evaluated region.

The differences obtained for comparing Figure 1a to Figure 1d can be explained by the greater spacing between pulses, that is, when the surface roughness is evaluated in Figure 1a, is also analyzing regions where there was no incidence of the laser beam, and therefore, have surface finishing typical of the material polished, finished surface of the final product. This does not happen, for example, on the samples of Figures 1b up to 1d, where the points are closer to each other.

In the sample shown in Figures 1b up to 1d, these isolated points produced by the laser pulse can not be observed, but only the change of the surface topography, because overlapping pulses and the laser welded area are more significant. It is unable to identify the exact points where there was the incidence of laser beam, but only a path of the laser beam, because of the joining of the fused areas.

It is found that for the lower scan rate (4 mm/s), lower energy used is that which produces the more number of points apart from each other, and better defined, having circular shapes with diameters that increase from the focal point to a stage where they do not become more evident. This diameter increase is due to the molten metal that moves from the center (the point of incidence of the beam) to

the edges, producing changes in height and depth in relation to the base metal, resulting thus in no volumetric variations arising from the evaporation of material, but the drag of liquid metal that generated splashing in the heat affected zone.

### 3.2. Open Circuit Potential (OCP)

Figure 2 presents the open circuit potential (OCP) as a function of the immersion time for the laser treated and non treated surfaces during a period of 17 h of immersion in PBS solution. The observed variation in the OCP indicates that the laser treated sample's susceptibility to pitting is dependent of the selected parameters.

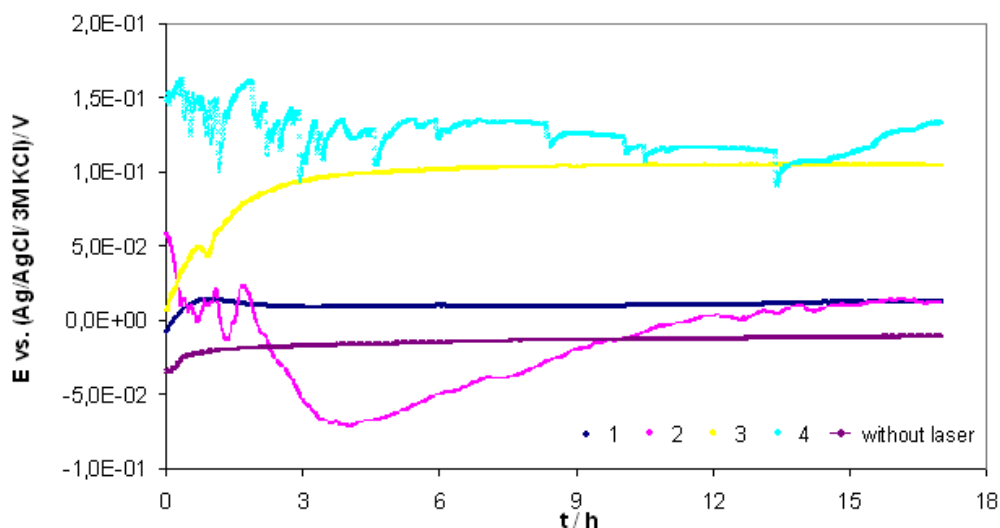


**Figure 2.** Corrosion potential in function of 17h of immersion in the PBS electrolyte.

As evidenced already in the first period of immersion for samples 2 and 4, showing frequent drops, that indicates the attack of the oxide layer. In the sample's 2 condition, after a period of approximately 4 h, the potential increases indicating the thickening or formation of a more homogeneous oxide surface film after the removal of defective areas.

The behaviour presented by sample 3 initially indicates a potential drop at about 1h of immersion, followed by an exponential increase in the potential, which maintains constant starting from 4 h to the end of the experiment.

For samples 1 and without laser shows similar behaviors, theirs corrosion potential reaches stabilization in the first periods of immersion.

Analyzing Figure 2 enables classify the pulse intensity as a parameter that causes the deleterious effect on the surfaces treated by Nd: YAG laser.

3.3. Electrochemical Impedance Spectroscopy (EIS)

The laser treatment significantly alters the microstructure and roughness of the stainless steel due to melting and rapid cooling of the surface, similar to what occurs in the laser welding of stainless steels [20-22]. This influences the susceptibility to localized corrosion, as it affects the semiconductor properties of the passive film.

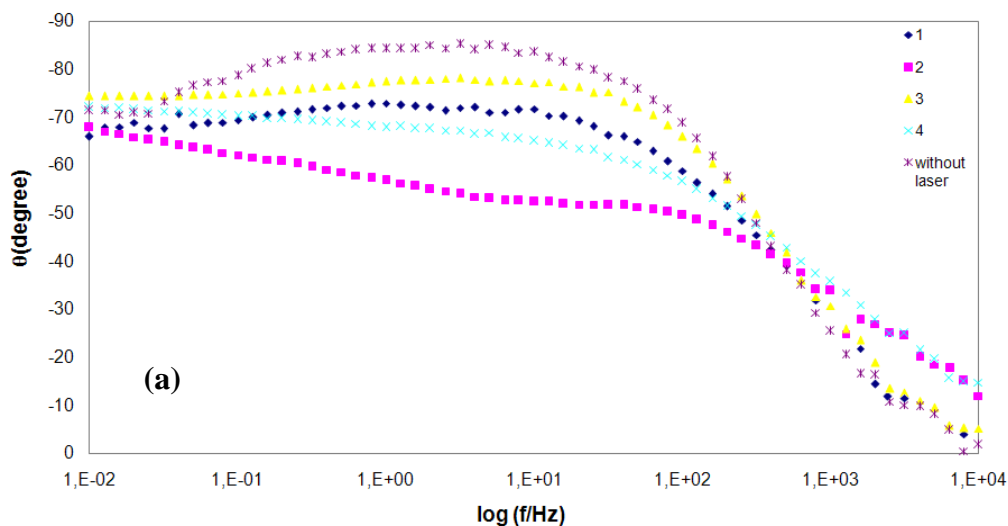


Figure 3. (a). Bode (phase angle) diagrams for laser treated and untreated ASTM F 139 SS surfaces, after OCP, in PBS solution.

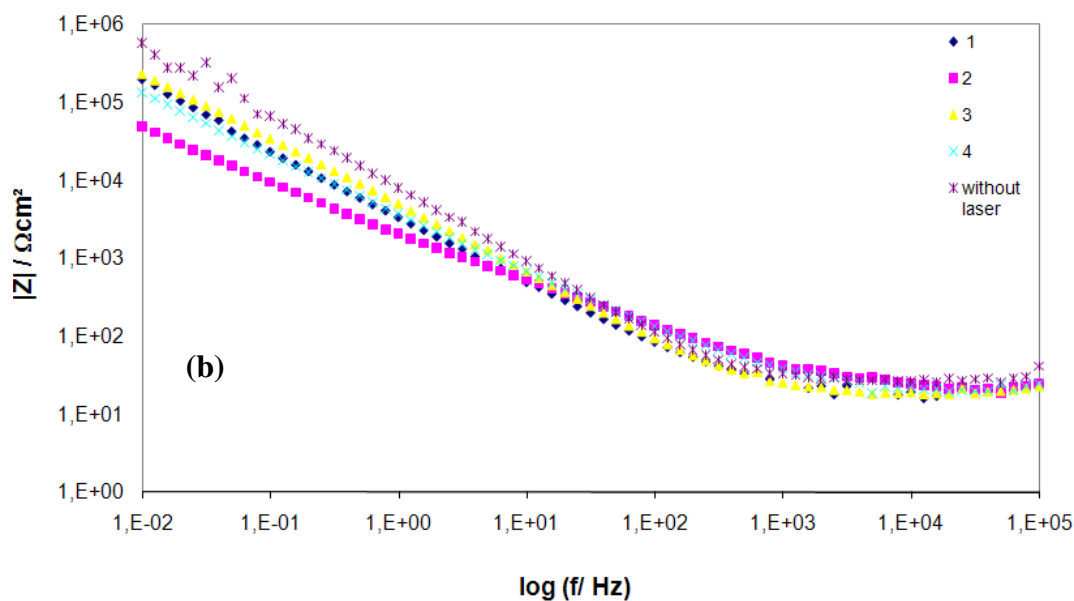


Figure 3. (b). Bode (Z Module) diagrams for laser treated and untreated ASTM F 139 SS surfaces, obtained after OCP, in PBS solution.

The EIS measurements on this biomaterial, treated and not treated by laser, immediately after 17 h of immersion in PBS solution are shown in Figure 3.

The Bode plots (phase angle) in Figure 3 (a) show phase angles between  $-65^\circ$  and  $-75^\circ$  at lower frequencies. High angles at low frequencies are typical of passive materials. At medium frequencies, the diagram presents a decrease in phase angle for samples 1, 3 and without laser treatment, whereas for samples 2 and 4 it increases continuously. This behaviour is changed at higher frequencies.

The Bode diagrams ( $Z$  modulus) shown in Figure 3 (b) represent the reproducibility obtained in the tests for each condition, and shows that this technique influences the impedance in the low frequencies region, being the lowest obtained for samples 2 and 4, followed by the samples 1 and 3, in comparison with samples without laser treatment. This fact shows a decrease in the protective ability of the film mainly for the samples treated with higher energies.

Figure 3 (c) presents the Nyquist plots for this biomaterial. It is evident the capacitive behavior for all tested conditions; being the less capacitive for samples 2 and 4 and the higher impedance values associated with stainless steel non treated.

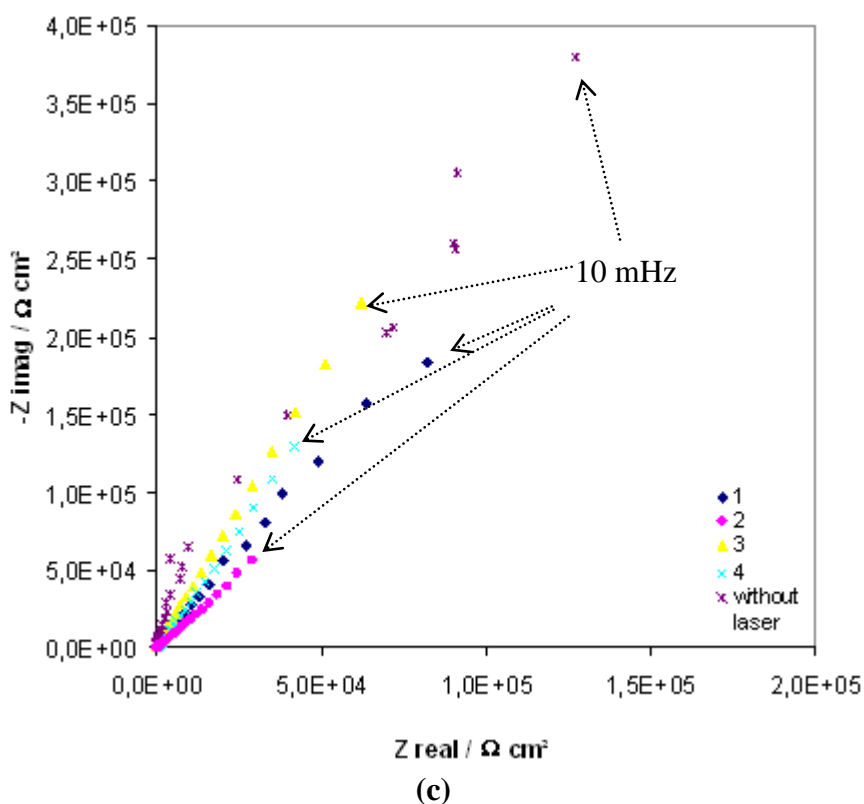


**Figure 3.** (c). Nyquist diagrams for laser treated and untreated ASTM F 139 SS surfaces, after OCP, in PBS solution.

### 3.4. Equivalent Electrical Circuits (EEC's)

Many equivalent electrical circuits have been tested to analyze the results of EIS, whose physical meaning could be related to the evaluated system. For each EIS curve was chosen the simple

model that allowed adjustment [23]. The circuit selected to adjust the results of the EIS is shown in Figure 4; for comparison reasons the blank surface was also evaluated.

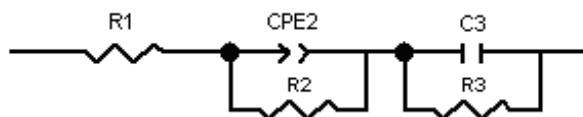


**Figure 4.** Equivalent electrical circuit proposed to characterize the passive layer of the ASTM F 139 SS for surfaces treated by laser and without laser.

The passive layer on the duplex stainless steels, characterized by the circuits, consists in an outermost layer, in contact with the electrolyte, which is more porous and composed primarily of iron oxides, compared to the innermost. The innermost layer, in contact with the substrate, which is compact and composed mainly of chromium oxide, being primarily responsible for the protection of the metallic substrate against corrosion [24- 27].

The values of the components of EEC, obtained by the settings of the EIS experimental results after 17 h of immersion at 37° C are shown on Table 2. In the published literature [28-29], the response at high frequencies has been proposed. At this work, CPE2 is a constant phase element, C3 is an ideal capacitor, R1 is the resistance of the electrolyte, R2 is the resistance of the outer oxide, R3 is the resistance of the inner oxide, and n2 refers to the power of the CPE2. The R2/CPE2 pair was associated to the oxide film-electrolyte interface, whereas the R3/C3 pair was related to the substrate-oxide film interface.

**Table 2.** Values obtained from fitting for the components of the equivalent electrical circuit shown in Figure 4.

	R1 (Ωcm <sup>2</sup> )	CPE2 (cm <sup>-2</sup> s <sup>-1</sup> Ω)	n2	R2 (Ω.cm <sup>2</sup> )	C3 (cm <sup>-2</sup> s <sup>-1</sup> Ω) <sup>n</sup>	R3 (Ω.cm <sup>2</sup> )
Laser (1)	25.0	8.00 x10 <sup>-5</sup>	0.761	31411	5.93 x10 <sup>-5</sup>	1.40 x10 <sup>6</sup>
Laser (2)	20.0	1.12 x10 <sup>-4</sup>	0.611	19864	2.51 x10 <sup>-4</sup>	1.65 x10 <sup>5</sup>
Laser (3)	18.55	1.10 x10 <sup>-4</sup>	0.777	26913	4.51 x10 <sup>-5</sup>	2.47 x10 <sup>6</sup>
Laser (4)	19.24	1.08 x10 <sup>-4</sup>	0.679	37000	1.24 x10 <sup>-4</sup>	7.67 x10 <sup>5</sup>
Without Laser	38.57	7.50 x10 <sup>-5</sup>	0.850	29030	4.97 x10 <sup>-5</sup>	1.06x10 <sup>6</sup>

The lower R3 values were associated with the samples treated by laser with higher intensity. This resistance was related to charge transfer at the oxide film-substrate interface and was much inferior comparing to the other types of treated surfaces.

The low R2 values for samples treated with the parameters 2 may be indicative of the formation of a porous oxide/hydroxide layer containing pores filled with the electrolyte. The n2 values, which indicated that the outer part of the oxide layer (oxide-electrolyte interface) was heterogeneous, suggested that laser treated samples possessed a more uneven surface, as shown on the images above. In addition, the higher n2 values were obtained by non treated surfaces.

Furthermore, the R3 values, which were 10 times greater for samples 1 and 3 or untreated samples than those of laser treated samples, showed that the inner substrate-oxide film interface of these surface were also less resistant to corrosion.

#### 4. CONCLUSIONS

The results indicated that the surface finishing of this stainless steel is affected by the laser parameters. The inferior values of scan rate and pulse energy produces the most visible points, and when increasing both, only the laser pathway is shown.

The Nd: YAG laser pulse intensity is the parameter that most affects the susceptibility to corrosion of this biomaterial. An increase in the laser pulse intensity increases its susceptibility to localized breakdown of its passive film.

#### References

1. Y. Okasaki, *Biomaterials*, 23 (2002) 2071.
2. D. F. Williams, *Mater. Sci.*, 6 (1976) 237.
3. L. L. Hench, *Mater. Sci.*, 5 (1975) 279.
4. J. M. Anderson, *Mater. Res.*, 31 (2001) 81.
5. M. Pourbaix, *Corros. Sci.*, 3 (1963) 239.
6. ABNT NBR 12932: 2010, Implantes para cirurgia – Materiais metálicos – Preparação de superfície e marcação.
7. A. Borruto, I. Taraschi, *Wear*, 184 (1995) 119.
8. T. Hong, M. Nagumo, *Corros. Sci.*, 39 (1997) 1665.
9. R. M. Patrikar, *Appl. Surf. Sci.*, 228 (2004) 213.
10. J. Qi, K. L. Wang, Y. M. Zhu, *J. Mater. Proc. Tec.*, 139 (2003) 273.
11. C. Leone, S. Genna, G. Caprino, I. De Iorio, *J. Mater. Proc. Tec.*, 210 (2010) 1293.
12. P. Bizi-Bandoki, S. Benayoun, S. Valette, B. Beaugiraud, E. Audouard, *Appl. Surf. Sci.* 257 (2011) 5213.
13. S. Valette, P. Steyer, L. Richard, B. Forest, C. Donnet, E. Audouard, *Appl. Surf. Sci.*, 252 (2006) 4696.
14. C. Soriano, J. Leunda, J. Lambarri, V. García-Navas, C. Sanz, *Appl. Surf. Sci.*, 257 (2011) 7101.
15. J. Diaci, D. Bračun, A. Gorkič, J. Možina, *Optics and Lasers in Eng.*, 49 (2011) 195.
16. E. F. Pieretti, I. Costa, *Electrochim. Acta*, 114 (2013) 838.
17. E. F. Pieretti, S. M. Manhobosco, L. F. P. Dick, S. Hinder, I. Costa, *Electrochim. Acta*, 124 (2014) 150.
18. E. F. Pieretti, R. P. Palatnic, T. P. Leivas, I. Costa, M. D. M. das Neves, *Int. J. Electrochem. Sci.*, 9 (2014) 2435.

19. E. F. Pieretti, I. Costa, R. A. Marques, T. P. Leivas, M. D. M. das Neves, *Int. J. Electrochem. Sci.*, 9 (2014) 3828.
20. G. A. Zhang, Y. F. Cheng, *Electrochim. Acta*, 55 (2009) 316.
21. M. Qian, J. N. DuPont, *Corros. Sci.*, 52 (2010) 3548.
22. Z. Feng, X. Cheng, C. Dong, L. Xu, X. Li, *Corros. Sci.* 52 (2010) 3646.
23. P. L. Bonora, F. Deflorian, L. Fedrizzi, *Electrochim. Acta*, 41, (1996) 1073.
24. M. Da Cunha Belo, M. Walls, N. E. Hakiki, J. Corset, E. Picquenard, G. Sagon, D. Noël, *Corros. Sci.*, 40 (1998) 447.
25. N. E. Hakiki, M. Da Cunha Belo, *J. Electrochem. Soc.*, 145 (1998) 3821.
26. N. E. Hakiki, S. Baudin, B. Rondot, M. Da Cunha Belo, *Corros. Sci.*, 37 (1995) 1809.
27. N. E. Hakiki, M. F. Montemor, M.G.S. Ferreira, M. Da Cunha Belo, *Corros. Sci.*, 42 (2000) 687.
28. K. Azumi, T. Ohtsuka, N. Sato, *Trans. Japan Inst. Metals*, 27 (1986) 382.
29. H. Ge, G. Zhou, W. Wu, *Appl. Surf. Sci.*, 211 (2003) 321.

© 2015 The Authors. Published by ESG ([www.electrochemsci.org](http://www.electrochemsci.org)). This article is an open access article distributed under the terms and conditions of the Creative Commons Attribution license (<http://creativecommons.org/licenses/by/4.0/>).